New search for ^{26}O

M. Fauerbach,[1,2] D. J. Morrissey,[2,3] W. Benenson,[1,2] B. A. Brown,[1,2]
M. Hellström,[2,*] J. H. Kelley,[1,2] R. A. Kryger,[1,2] R. Pfaff,[1,2] C. F. Powell,[2,3] and B. M. Sherrill[1,2]
[1]*Department of Physics and Astronomy, Michigan State University, East Lansing, Michigan 48824*
[2]*National Superconducting Cyclotron Laboratory, Michigan State University, East Lansing, Michigan 48824*
[3]*Department of Chemistry, Michigan State University, East Lansing, Michigan 48824*
(Received 27 July 1995)

An attempt was made to find the very neutron-rich isotope ^{26}O among the fragmentation products of a 90 MeV/nucleon ^{40}Ar beam. This isotope has been predicted to be bound but was not observed in a previous experiment by Guillemaud-Mueller *et al.* As part of the search, the momentum distributions of all the oxygen isotopes in the range from ^{17}O to ^{24}O were carefully determined so that the optimum separator setting for ^{26}O could be used. From an extrapolation of the counting rates of the lighter oxygen isotopes, we expected to observe several hundred events of ^{26}O during the measurement. However, no events could be attributed to ^{26}O, thus indicating the particle instability of this isotope. The results for the production cross sections of 72 neutron-rich isotopes, ranging from ^{38}P to ^{11}B, are presented and compared to predictions.

PACS number(s): 27.30.+t, 25.70.Mn, 21.10.Dr

I. INTRODUCTION

The exact locations of the boundaries of particle stability, the so-called driplines, are interesting from an experimental as well as from a theoretical standpoint. Many theoretical models, both macroscopic and microscopic, predict the ground state masses as well as the one- and two-particle separation energies, and also predict the driplines. The exact location of the neutron dripline is only known experimentally for the lightest elements and, therefore, experimental studies to establish the limits of particle stability remain important. The nuclei close to the driplines are also of particular interest as they should show some unique properties due to their very small one- or two-particle separation energies. This is especially true on the neutron-rich side, where the influence of the Coulomb force on the mean field is small. As an example, ^{11}Li has a very large nuclear matter radius that has been interpreted as evidence for a halo structure. It is expected that many more of these one- and two-neutron halo nuclei will be found as one approaches the limits of particle stability.

Some disagreement, particularly in the sodium region, between the experimentally determined values and the theoretical estimates for the binding energies of the most neutron-rich isotopes has been noted by several authors [1,2]. With the use of large scale computer codes the disagreement has lessened in recent years, although there are still several regions where the models do not agree with the experimental findings or with each other. The predictions of several models for the particle stability of ^{26}O can be summarized in terms of the binding energy curves for oxygen isotopes shown in Fig. 1. The experimental data (solid circles) are compared with several predictions: the global prediction of Möller and Nix [3] (MN) and two different shell-model calculations, labeled as *W-WBMB* and *SDPOTA*. W refers to Wildenthal's USD interaction [4] obtained from a fit of the two-body matrix elements to binding energy and excitation energy data in the $0s1d$ shell ($N,Z=8,20$). *SDPOTA* [6] is a more recent interaction obtained from a fit of density-dependent one-boson exchange potential strengths to the same set of energy data. *W* has effectively 47 parameters whereas *SDPOTA* is more constrained with 14 potential strength and three single-particle energy parameters. *WBMB* is an addition and extension of *W* into the fp shell [5]. Both *W* and *SDPOTA* do about equally well in reproducing the known experimental binding energies of the oxygen isotopes.

The global model of Möller and Nix predicts ^{26}O and even the doubly magic nucleus ^{28}O to be stable, while the global systematics by Audi and Wapstra [7] predict ^{24}O as the heaviest bound oxygen isotope with ^{26}O unbound by 50 keV. The *W-WBMB* calculations also predict ^{26}O to be bound by about 1 MeV. The *SDPOTA* calculation, on the other hand, predicts ^{26}O to be unbound, but only by 20 keV. These differences are an indication of the rather large model dependence which exists in the theoretical extrapolation to the most exotic nuclei. The odd-even nuclei ^{25,27}O are known to be unbound against one neutron decay [7], in agreement with all of the model calculations.

The difficulty of predicting the binding energies of the heaviest oxygen isotopes, for both global- and shell-model calculations, can be easily understood in the simple j-j coupling limit. In Fig. 2 the effective neutron separation energy (S_n) is shown as a function of neutron number. As can be clearly seen, S_n changes slowly with neutron number due to the relatively weak average interaction between the valence neutrons. Between $N=8$ and 14, the neutrons fill the $d_{5/2}$ orbit, which is bound by about 4 MeV. This, together with the attractive pairing energy, provides the sharp increase in binding energy observed between $N=8$ and $N=14$. At $N=15$

*Present address: Gesellschaft für Schwerionenforschung, D-64220 Darmstadt, Germany.

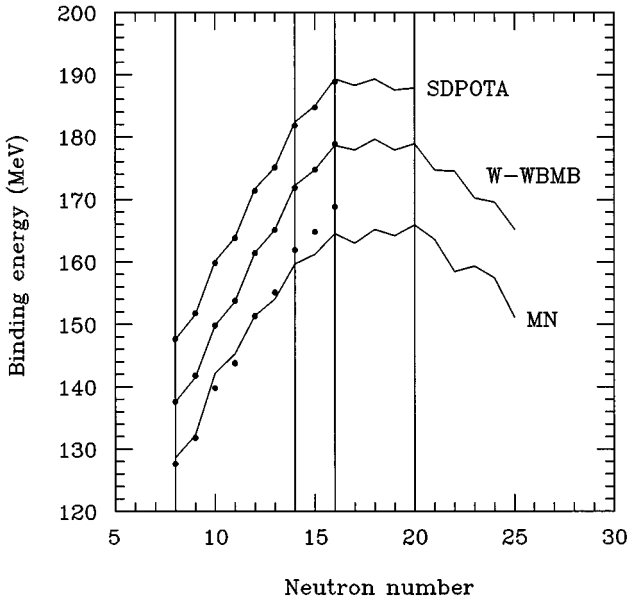

FIG. 1. Measured binding energies of the ground states of oxygen isotopes (solid circles) compared to several model predictions (solid lines). For display purposes 10 MeV has been added to the *W-WBMB* comparison and 20 MeV to the *SDPOTA* comparison.

and 16 the neutrons fill the $s_{1/2}$ orbit which is less bound than the $d_{5/2}$. Thus one sees a smaller increase in the binding energy at this point. From $N=16$ up to 20 the neutrons fill the $d_{3/2}$ orbit which has close to zero binding energy, and the total binding energy curve becomes flat. This slow change in separation energy with the neutron number leads to difficulty predicting whether a nucleus is bound or unbound. Beyond $N=20$ the neutrons have to go into the next major shell (pf orbits) which are unbound, hence the binding energy curve decreases beyond this point.

Figure 3 shows the two-neutron separation energies for the known isotopes in this region from the compilation of Audi and Wapstra [7]. As clearly shown in this figure, all the

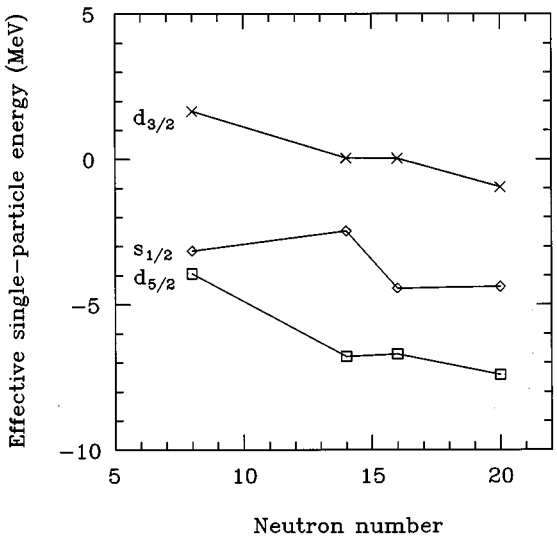

FIG. 2. The effective neutron separation energy as a function of neutron number according to the shell-model calculations.

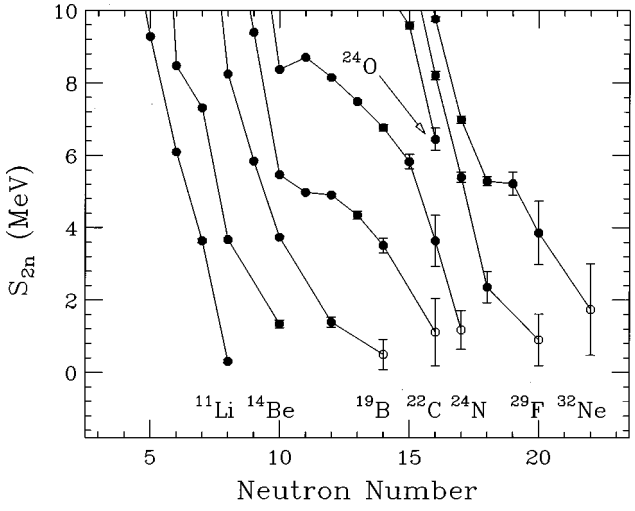

FIG. 3. Two-neutron separation energies for various light isotopes as given by Ref. [7]. The solid circles indicate measured values, whereas the open circles show estimates from systematics (see Ref. [7] for details) for isotopes that are known to exist, but for which no direct mass measurement has been performed.

elements near oxygen have several bound isotopes with two-neutron separation energies that are much smaller than that of ^{24}O. The heaviest experimentally known oxygen isotope is ^{24}O, and a previous attempt to synthesize ^{26}O using a ^{48}Ca beam was not successful [2]. In the present work a new investigation of the particle stability of ^{26}O was carried out with greater sensitivity than that previously employed.

II. EXPERIMENTAL PROCEDURE

A 90 MeV/nucleon ^{40}Ar beam from the K1200 cyclotron at the National Superconducting Cyclotron Laboratory irradiated a 190 mg/cm^2 ^{9}Be target located at the medium acceptance target position of the A1200 fragment separator [8]. The average beam intensity, using the superconducting ECR ion source, was about 20 pnA. The momentum acceptance of the A1200 was $\pm 1.5\%$ and the angular acceptances were ± 10 mrad in θ and ± 20 mrad in ϕ. The experimental setup and analysis procedures used for this experiment were similar to those described in Ref. [9] and will only be briefly described. The time of flight for each particle was measured over the 14 m flight path between a plastic scintillator located at the first dispersive image and a semiconductor detector located at the focal plane of the A1200. The magnetic rigidity of each particle ($B\rho$), which is linearly related to its momentum, was obtained by combining a position measurement, using parallel plate avalanche counters, at the second dispersive image of the separator with NMR measurements of the A1200 dipole fields. The reaction products that reached the A1200 focal plane were implanted into a four-element silicon detector telescope. The telescope consisted of two thin (100 and 75 μm) ΔE and two thicker (500 and 1000 μm) E detectors, each with a 300 mm^2 active area. The simultaneous measurements of ΔE-E, the magnetic rigidity, and the time of flight for each particle provided an unambiguous identification of the atomic number, charge state, and mass of the produced fragments.

The relative beam current was monitored continuously by four small PIN diodes mounted around the target position to normalize data obtained at different magnetic rigidity settings. A small irreproducibility in the absolute beam current was found in the off-line analysis. Therefore, the beam intensity was carefully measured in subsequent short runs along with the yields of a few products. The cross sections for these products were calculated and used to renormalize the relative cross sections determined in the long experiment.

In order to map out the (parallel) momentum distributions of the fragmentation products and provide the production yields (see Ref. [9] for details), the magnetic rigidity of the separator was varied stepwise over the range $B\rho = 2.96$–4.31 Tm. The momentum distributions of the lighter oxygen isotopes were monitored online so that the optimum separator setting for ^{26}O could be inferred independently of any model calculations, an improvement over the previous experiment. Once the optimum setting was determined, an energy loss degrader (^{9}Be, 47 mg/cm^2) was inserted at the intermediate focal plane of the A1200 to cut down the range of atomic numbers of the fragments reaching the final focus. The fact that ^{26}O was centered at the intermediate image and the final focus of the A1200 was also verified on line. This was done by measuring the positions of ^{19}C and ^{20}C fragments (which span ^{26}O in A/Q) at the intermediate focus and by measuring the energy loss of all the fragments versus their position at the final focus.

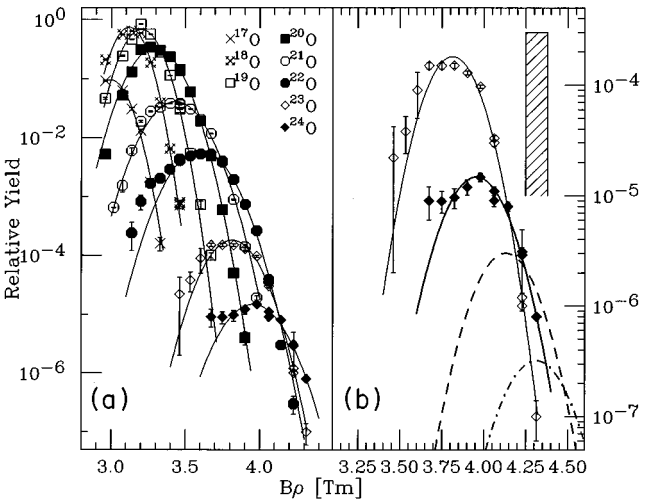

FIG. 4. (a) Measured relative production yield as a function of the magnetic rigidity, which is linearly related to the fragment momentum, for eight different oxygen isotopes ranging from ^{17}O to ^{24}O. The solid lines are Gaussian fits to the data. (b) An expanded version showing only the measured values for ^{23,24}O. The dashed line indicates the expected momentum distribution for ^{25}O, which is unbound against one neutron decay. The dash-dotted line shows the expected momentum distribution for ^{26}O, and the hatched area shows the acceptance of the A1200 at one specific setting (see text for details).

III. RESULTS AND DISCUSSION

The main objective of the experiment was to determine whether or not ^{26}O is particle unbound. To make this determination, the momentum distributions of many neutron-rich fragments were carefully determined. This information was then used to determine production cross sections of these fragments and to find the optimum separator setting for ^{26}O. The results of these measurements will be discussed and compared to the predictions of a semiempirical parametrization [11].

A. Momentum distributions and fragmentation cross sections

The momentum distributions of eight different oxygen isotopes in the range from ^{17}O to ^{24}O from the fragmentation of ^{40}Ar are shown in Fig. 4. Notice that these distributions span approximately 7 orders of magnitude in relative production yield. As can be seen in Fig. 4, the momentum distributions of the oxygen fragments are well described by Gaussian functions. Since the main objective of the present experiment was to produce a very exotic nucleus, a relatively thick target was used to optimize the production rate of this nucleus. Dufour *et al.* [10] have shown that the target thickness introduces an increase in the width of the momentum distribution due to the difference in energy loss of projectile and fragment. In the extreme case in which the fragment is produced at either the front or the back of the target, the differential energy loss creates an almost rectangular momentum distribution, whose width increases in proportion to the target thickness. In principle the two different components can be separated to give a nuclear reaction momentum width. However, since the unwanted effect from the target thickness was so large in the present case, the nuclear reaction widths were not deconvoluted.

Because the production cross sections are expected to change very little due to the target thickness, the production cross sections were obtained and compared to the semiempirical parametrization (EPAX) by Sümmerer *et al.* [11]. The absolute isotopic cross sections were obtained by integrating the fitted Gaussian distributions over momentum and normalizing the results by the incoming particle flux and the acceptance of the A1200. The incoming particle flux was measured between runs with a Faraday Cup, and the beam current was monitored during the run using four PIN diodes mounted around the target position. The acceptance for each individual isotope was calculated with the code LISE [12].

The absolute production cross sections for 72 neutron-rich isotopes ranging from ^{38}P to ^{11}B were determined and are shown in Fig. 5. The overall agreement between the measured data and predictions of the semiempirical formula EPAX is good. However, slight deviations between the measured and predicted cross sections are present. In Fig. 6, the cross sections for the oxygen isotopes are shown in more detail. Again, the overall agreement between the experimental data and the prediction is good, although the measured cross sections indicate a slightly different functional form for the isotopic yield than that used by EPAX. A similar trend can be seen in Fig. 5 for all isotopes with $Z < 12$. These, and other new data for light residues from fragmentation reactions could be used to refit the parameters of the EPAX formula to provide even better predictions of the cross sections.

The extrapolation of the expected counting rate for ^{26}O from the cross sections of the lighter oxygen isotopes is indicated in Fig. 6. The EPAX prediction is shown by the solid line. However, due to the systematic difference mentioned

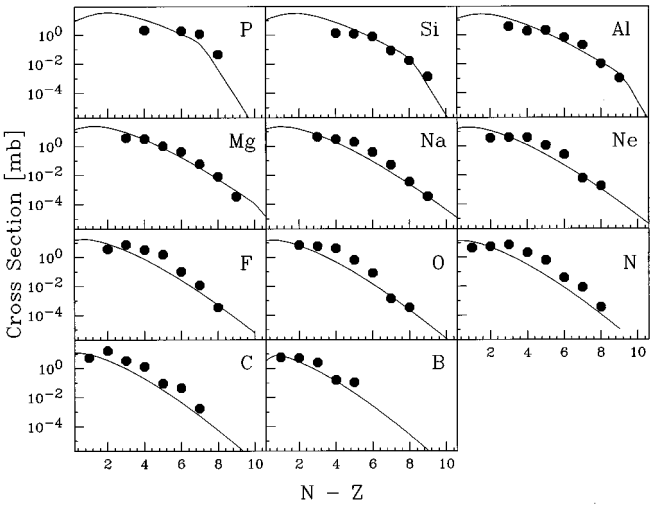

FIG. 5. Measured reaction cross sections for neutron-rich isotopes (solid points), ranging from ^{38}P to ^{11}B. The full line indicates the predictions of the semiempirical formula EPAX [11].

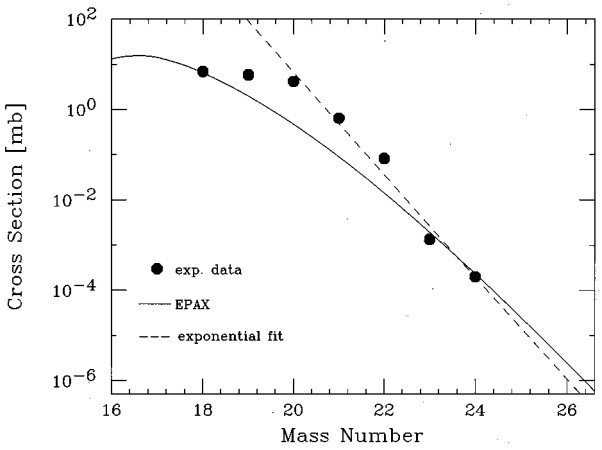

FIG. 6. Measured reaction cross sections for several oxygen isotopes (solid points), ranging from ^{18}O to ^{24}O. The full line indicates the predictions of the semiempirical formula EPAX [11], and the dashed line is an exponential fit to the experimental data. The extrapolated production cross sections for ^{26}O agree within a factor of 2.

above, a simple exponential fit to the most neutron-rich oxygen fragments was also used. Even though the curves have clearly different shapes, they predict very similar cross sections for ^{26}O, namely 2.43 nb (EPAX) and 1.07 nb (exponential fit).

B. The search for ^{26}O

The tuned setting of the A1200 during the search for ^{26}O is indicated in Fig. 4 by the hatched area that corresponds to the momentum acceptance of the A1200 during the long run. After 36 h of data collection at this one setting, 2132 events were identified as ^{24}O, approximately an order of magnitude more than the previous experiment [2], without a single event that could be attributed to ^{26}O. Using this yield of ^{24}O and the two cross section extrapolations (see previous section) of the yields of the lighter oxygen isotopes, we predict that approximately 400 or 800 events of ^{26}O should have been observed. The present data correspond to an upper limit on the production cross section for ^{26}O of 7 pb at a 90% confidence level. The expected momentum distribution for ^{26}O from the EPAX extrapolation is indicated by the dash dotted line in Fig. 4(b).

As a large effort was put into assuring that the particles of interest were centered at both the intermediate and final focus of the A1200, this result indicates that the lifetime of ^{26}O must indeed be appreciably shorter than the central flight time through the separator (approximately 188 ns). We interpret this to mean that ^{26}O is not particle stable and that ^{24}O is, in fact, the heaviest bound oxygen isotope.

IV. CONCLUSIONS

The present study has confirmed the previous finding that ^{26}O is particle unstable, with an increase in the confidence level of more than 1 order of magnitude, thus making ^{24}O the heaviest bound oxygen isotope.

The study also showed that the measured cross sections of 72 neutron-rich fragments are in good agreement with the predictions of the semiempirical parametrization EPAX. Slight deviations occur, however, for fragments that experienced the largest mass losses. The data seem to indicate a different functional form for the isotopic distributions than used by EPAX for these fragments.

ACKNOWLEDGMENTS

This work was supported by the National Science Foundation under Grant Nos. PHY-92-14922 and PHY 94-03666.

[1] J.M. Wouters, R.H. Kraus, D.J. Vieira, G.W. Butler, and K.E.G. Löbner, Z. Phys. A **331**, 229 (1988).

[2] D. Guillemaud-Mueller, J.C. Jacmart, E. Kashy, A. Latimier, A.C. Mueller, F. Pougheon, A. Richard, Yu.E. Penionzhkevich, A.G. Arthuk, A.V. Belozyorov, S.M. Lukyanov, R. Anne, P. Bricault, C. Détraz, M. Lewitowicz, Y. Zhang, Yu.S. Lyutostansky, M.V. Zverev, D. Bazin, and W.D. Schmidt-Ott, Phys. Rev. C **41**, 937 (1990).

[3] P. Möller and J.R. Nix, At. Data Nucl. Data Tables **39**, 221 (1988).

[4] B.H. Wildenthal, in *Progress in Particle and Nuclear Physics*, edited by D.H. Wilkinson (Pergamon, Oxford, 1984), Vol. 11, p. 5.

[5] E.K. Warburton, J.A. Becker, and B.A. Brown, Phys. Rev. C

41, 1147 (1990).
[6] B.A. Brown, W.A. Richter, R.E. Julies, and B.H. Wildenthal, Ann. Phys. **182**, 191 (1988).
[7] G. Audi and A.H. Wapstra, Nucl. Phys. **A565**, 1 (1993).
[8] B.M. Sherrill, D.J. Morrissey, J.A. Nolen, Jr., and J.A. Winger, Nucl. Instrum. Methods B **56**, 1106 (1991).
[9] R. Pfaff, D.J. Morrissey, M. Fauerbach, M. Hellström, J.H. Kelley, R.A. Kryger, B.M. Sherrill, M. Steiner, J.S. Winfield, J.A. Winger, and B.M. Young, Phys. Rev. C **51**, 1348 (1995).
[10] J.P. Dufour, R. Del Moral, H. Emmermann, F. Hubert, D. Jean, C. Poinot, M.S. Provikoff, A. Fleury, H. Delagrange, and K.-H. Schmidt, Nucl. Instrum. Methods A **248**, 267 (1986).
[11] K. Sümmerer, W. Brüchle, D.J. Morrissey, M. Schädel, B. Szweryn, and Yang Weifan, Phys. Rev. C **42**, 2546 (1990).
[12] D. Bazin (unpublished).